



Simulation of Single Phase Multilevel Inverter Topology for Distributed Energy Resources Using Multi Inputs

B. Suresh Kumar¹, GantaJoga Rao²

M.Tech Scholar, Dept. of EEE, Chirala Engineering College, Chirala, India¹

Associate Professor, Dept. of EEE, Chirala Engineering College, Chirala, India²

ABSTRACT: In the microgrid system, single-phase inverter is usually used for the distributed energy resource (DER). To reduce conversion losses, removing the transformer and reducing power devices will bring down the cost and size of the converter. The objective of this paper is to build simulation of seven level multistring inverter topology for DERs based DC to AC system. In this paper, a high step-up converter is used as front-end stage to improve the conversion efficiency of conventional boost converters and to stabilize the output DC voltage of various DERs such as PV and fuel cell modules for use with the simplified multilevel inverter. Seven level inverter requires only six active switches instead of the eight required in the conventional cascaded H-bridge inverter. In addition, two active switches are operated under line frequency. The simulated seven level string inverter topology offers strong advantages such as improved output waveforms, small filter size, and low magnetic interference and harmonic distortion. Simulation results show the effectiveness of the proposed solution.

Keywords: DC/AC power conversion, multilevel inverter.

I. INTRODUCTION

In light of public concern about global warming and climate change, much effort has been focused on development of environmentally friendly distributed energy resources (DERs). For delivering premium electric power in terms of high efficiency, reliability, and power quality, integrating interface converters of DERs such as photovoltaic, wind power, microturbines, and fuel cells into the microgrid system has become a critical issue in recent years [1]-[4]. In such systems, most DERs usually supply a DC voltage that varies in a wide range according to various load conditions. Thus, a DC/AC power processing interface is required and is compliant with residential, industrial, and utility grid standards [4]-[7]. Various converter topologies have been developed for DERs [7]-[16] that demonstrate effective power flow control performance whether in grid-connected or stand-alone operation. Among them, solutions that employ high-frequency transformers or make no use of transformers at all have been investigated to reduce size, weight, and expense. For low-medium power applications, international standards allow the use of grid-connected power converters without galvanic isolation, thus allowing so-called “transformerless” architectures [7], [12]. Furthermore, as the output voltage level increases, the output harmonic content of such inverters decreases, allowing the use of smaller and less expensive output filters. As a result, various multilevel topologies are usually characterized by a strong reduction in switching voltages across power switches, allowing the reduction of switching power losses and electromagnetic interference (EMI) [8], [11]. A single-phase multistring five-level inverter integrated with an auxiliary circuit was recently proposed for DC/AC power conversion [12], [13]. This topology used in the power stage offers an important improvement in terms of lower component count and reduced output harmonics. Unfortunately, high switching losses in the additional auxiliary circuit caused the efficiency of the multistring five-level inverter to be approximately 4% less than that of the conventional multistring three-level inverter [13]. In [14], a novel isolated single-phase inverter with generalized zero vectors (GZV) modulation scheme was first presented to simplify the configuration. However, this circuit can still only operate in a limited voltage range for practical applications and suffer degradation in the overall efficiency as the duty cycle of the DC-side switch of the front-end conventional boost converter approaches unity [6], [14]. Furthermore, the use of isolated transformer with multi-windings of the GZV based inverter results in the larger size, weight, and additional expense [14]. To overcome the above-mentioned problem, the objective of this paper is to study a newly-constructed transformerless five-level

International Journal of Advanced Research in Electrical, Electronics and Instrumentation Engineering

(An ISO 3297: 2007 Certified Organization)

Vol. 2, Issue 12, December 2013

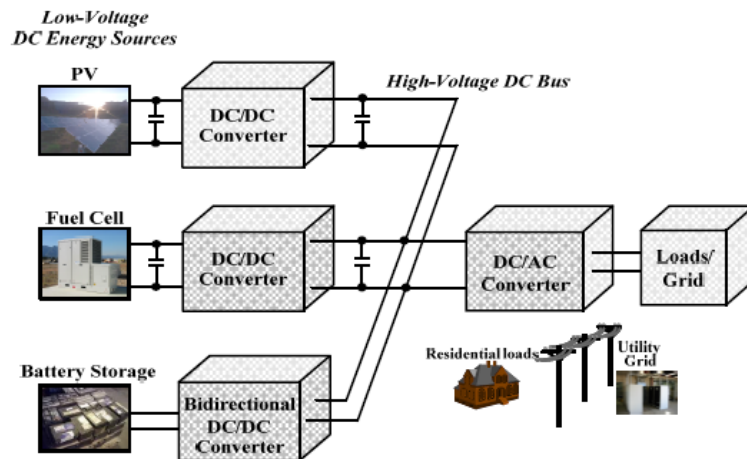


Fig. 1 Configuration of multistring inverter for various DERs application

multistring inverter topology for DERs. In this paper, the foresaid GZV-based inverter is reduced to a multistring multilevel inverter topology that requires only six active switches instead of the eight required in the conventional cascaded H-bridge (CCHB) multilevel inverter [16]. In addition, among them, two active switches are operated under line frequency. In order to improve the conversion efficiency of conventional boost converters, a high step-up converter [26] is also introduced as a front-end stage to stabilize the output DC voltage of each DER module for use with the simplified multilevel inverter. The newly-constructed inverter topology offers strong advantages such as improved output waveforms, smaller filter size, and lower EMI and total harmonic distortion (THD). In this paper, the operating principle of the developed system is described, and a simulation is constructed for verifying the effectiveness of the topology.

II. SYSTEM CONFIGURATION OF OPERATION PRINCIPLES

A general overview of different types of photovoltaic (PV) modules or fuel cell inverters is given in [9]. This paper presents a multistring multilevel inverter for DERs application. The multistring inverter shown in Fig. 1 is a further development of the string inverter, whereby several strings are interfaced with their own DC/DC converter to a common inverter. This centralized system is beneficial because each string can be controlled individually. Thus, the operator may start his own PV/fuel cell power plant with a few modules. Further enlargements are easily achieved because a new string with a DC/DC converter can be plugged into the existing platform, enabling a flexible design with high efficiency [9]. The single-phase multistring multilevel inverter topology used in this study is shown in Fig. 2. This topology configuration consists of two high step-up DC/DC converters connected to their individual DC bus capacitor and a simplified multilevel inverter. Input sources, DER module 1, and DER module 2 are connected to the inverter followed a linear resistive load through the high step-up DC/DC converters. The studied simplified five-level inverter is used instead of a conventional phase disposition (PD) pulse width modulated (PWM) inverter because it offers strong advantages such as improved output waveforms, smaller filter size, and lower electromagnetic interference and THD. It should be noted that, by using the independent voltage regulation control of the individual high step-up converter, voltage balance control for the two bus capacitors C_{bus1} , C_{bus2} can be achieved naturally.

A. High Step-Up Converter Stage:

In this study, high step-up converter topology is introduced to boost and stabilize the output DC voltage of various DERs such as PV and fuel cell modules for employment of the proposed simplified multilevel inverter. The architecture of a high step-up converter initially introduced from, depicted in Fig. 2, and is composed of different converter topologies: boost, flyback, and a charge pump circuit. The coupled inductor of the high step-up converter in Fig. 2 can be modelled as an ideal transformer, a magnetizing inductor, and a leakage inductor. According to the voltage seconds balance condition of the magnetizing inductor, the voltage of the primary winding can be derived as

International Journal of Advanced Research in Electrical, Electronics and Instrumentation Engineering

(An ISO 3297: 2007 Certified Organization)

Vol. 2, Issue 12, December 2013

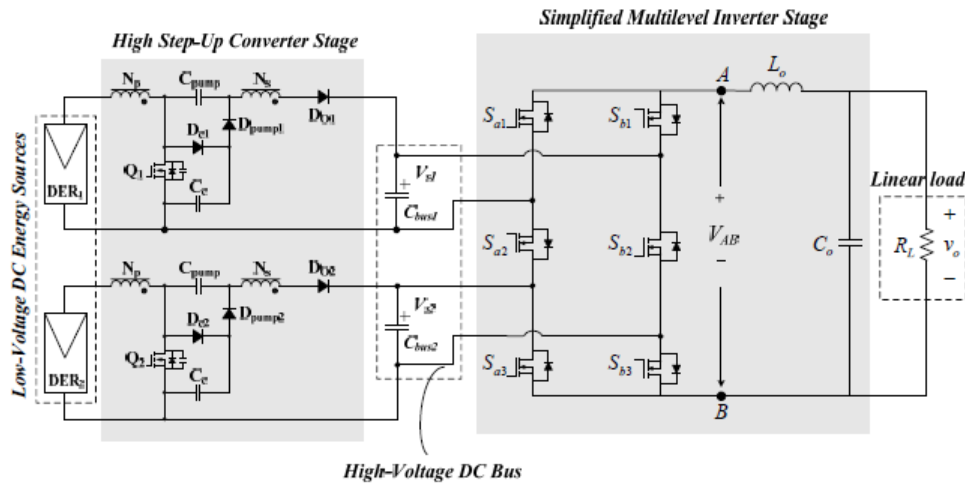


Fig. 2 Single-phase multistring five-level inverter topology

where V_{in} represents each the low-voltage DC energy inputsources, and voltage of the secondary winding is similar to that of the boost converter, the voltage of the charge-pump capacitor C_{pump} and clamp capacitor C_c can be expressed as

$$v_{pri} = V_{in} \cdot \frac{D}{(1-D)} \quad (1)$$

Hence, the voltage conversion ratio of the high step-up converter, named input voltage to bus voltage ratio, can be derived as [26]

$$v_{sec} = \frac{N_s}{N_p} \cdot v_{pri} = \frac{N_s}{N_p} \cdot V_{in} \cdot \frac{D}{(1-D)} \quad (2)$$

B. Simplified Multilevel Inverter Stage

To assist in solving problems caused by cumbersome power stages and complex control circuits for conventional multilevel inverters, this work reports a new single-phase multistring topology, presented as a new basic circuitry in Fig. 3. Referring to Fig. 2, it should be assumed that, in this configuration the two capacitors in the capacitive voltage divider are connected directly across the DC bus, and all switching combinations are activated in an output cycle. The dynamic voltage balance between the two capacitors is automatically controlled by the preceding high step-up converter stage. Then, we can assume $V_{s1} = V_{s2} = V_s$.

This topology includes six power switches—two fewer than the CCHB inverter with eight power switches—which drastically reduces the power circuit complexity and simplifies modulator circuit design and implementation. The PD PWM control scheme is introduced to generate switching signals and to produce five output-voltage levels: zero, V_s , $2V_s$, $-V_s$, and $-2V_s$. This inverter topology uses two carrier signals and one reference to generate PWM signals for the switches. The modulation strategy and its implemented logic scheme in Fig. 4(a) and (b) are a widely used alternative for phase disposition modulation. With the exception of an offset value equivalent to the carrier signal amplitude, two comparators are used in this scheme with identical carrier signals V_{tri1} and V_{tri2} to provide high-frequency switching signals for switches S_{a1} , S_{b1} , S_{a3} and S_{b3} . Another comparator is used for zero crossing detection to provide line-frequency switching signals for switches S_{a2} and S_{b2} .

For convenient illustration, the switching function of the switch in Fig. 3 is defined as follows: Table I. lists switching combinations that generate the required five output levels. The corresponding operation modes of the multilevel inverter stage are described clearly as follows:

$$v_{Cp} = v_{Cc} = V_{in} \cdot \frac{1}{(1-D)} \quad (3)$$

International Journal of Advanced Research in Electrical, Electronics and Instrumentation Engineering

(An ISO 3297: 2007 Certified Organization)

Vol. 2, Issue 12, December 2013

$$\frac{V_{si}}{V_{in}} = \left(2 + \frac{N_s}{N_p} \cdot D \right) \bigg/ (1 - D) \bigg|_{i=1,2} \quad (4)$$

- (1) Maximum positive output, $2V_s$: Active switches S_{a2} , S_{b1} , and S_{b3} are on; the voltage applied to the L-C output filter is $2V_s$.
- (2) Half-level positive output, $+V_s$: This output condition can be induced by two different switching combinations. One switching combination is such that active switches S_{a2} , S_{b1} , S_{a3} are on; the other is such that active switches S_{a2} , S_{a1} , S_{b3} are on. During this operating stage, the voltage applied to the L-C output filter is $+V_s$.
- (3) Zero output, 0: This output condition can be formed by either of the two switching structures. Once the left or right switching leg is on, the load will be short-circuited, and the voltage applied to the load terminals is zero.
- (4) Half-level negative output, $-V_s$: This output condition can be induced by either of the two different switching combinations. One switching combination is such that active switches S_{a1} , S_{b2} , S_{b3} are on; the other is such that active switches S_{a3} , S_{b1} , S_{b2} are on.
- (5) Maximum negative output, $-2V_s$: During this stage, active switches S_{a1} , S_{a3} , and S_{b2} are on, and the voltage applied to the

L-C output filter is $-2V_s$. In these operations, it can be observed that the open-circuit voltage stress of the active power switches S_{a1} , S_{a3} , S_{b1} , S_{b3} are equal to input voltage V_s ; moreover, the main active switches S_{a2} and S_{b2} are operated at the line frequency. Hence, the resulting switching losses of the new topology are reduced naturally, and the overall conversion efficiency is improved. To verify the feasibility of the single-phase five-level inverter, a widely used software program PSIM is applied to simulate the circuit according to the previously mentioned operation principle. The control signal block is shown in Fig. 4; $m(t)$ is the sinusoidal modulation signal.

$$S_{aj} = \begin{cases} 1, & S_{aj} \text{ ON} \\ 0, & S_{aj} \text{ OFF} \end{cases}, j = 1, 2, 3$$

$$S_{bj} = \begin{cases} 1, & S_{bj} \text{ ON} \\ 0, & S_{bj} \text{ OFF} \end{cases}, j = 1, 2, 3 \quad (5)$$

Both V_{tri1} and V_{tri2} are the two triangular carrier signals. The peak value and frequency of the sinusoidal modulation signal are given as $m_{peak} = 0.7$ and $f_m = 60\text{Hz}$, respectively. The peak-to-peak value

of the triangular modulation signal is equal to 1, and the switching frequency f_{tri1} and f_{tri2} are both given as 1.8kHz . The two input voltage sources feeding from the high step-up converter is controlled at 100V , i.e. $V_{s1} = V_{s2} = 100\text{V}$. The simulated waveform of the phase voltage with five levels is shown in Fig. 5. The switch voltages of S_{a1} , S_{a2} , S_{a3} , S_{b1} , S_{b2} , and S_{b3} are all shown in Fig. 6. It is evident that the voltage stresses of the switches S_{a1} , S_{a3} , S_{b1} , and S_{b3} are all equal to 100V , and only the other two switches S_{a2} , S_{b2} must be 200V voltage stress.



International Journal of Advanced Research in Electrical, Electronics and Instrumentation Engineering

(An ISO 3297: 2007 Certified Organization)

Vol. 2, Issue 12, December 2013

Table – I Switching Combination

S_{a1}	S_{a2}	S_{a3}	S_{b1}	S_{b2}	S_{b3}	V_{AB}
0	1	0	1	0	1	$2V_S$
0	1	1	1	0	0	V_S
1	1	0	0	0	1	V_S
1	1	1	0	0	0	0
0	0	0	1	1	1	0
1	0	0	0	1	1	$-V_S$
0	0	1	1	1	0	$-V_S$
1	0	1	0	1	0	$-2V_S$

C. Comparison with CCHB inverter

The average switching power loss P_s in the switch caused by these transitions can be defined as where $t_{c(on)}$ and $t_{c(off)}$ are the turn-on and turn-off crossover intervals, respectively; V_{DS} is the voltage across the switch; and I_o is the entire current which flows through the switch. Compared with the CCHB circuit topology as shown in Fig.7, the voltage stresses of the eight switches of the CCHB inverter are all equal to V_s . For simplification, both the proposed circuit and CCHB inverter are operated at the same turn-on and turn-off crossover intervals and at the same load I_o . Then, the average switching power loss P_s is proportional to V_{DS} and f_{s} as $P_s \propto V_{DS} f_{s}$. According to Eq. (8), the switching losses of the CCHB inverter from eight switches can be obtained as $P_{s,CCHB} = 8 I_o V_s f_{s}$. Similarly, the switching power loss of the proposed single phase five-level inverter due to six switches can also be obtained as $P_{s,proposed} = 6 I_o V_s f_{s}$. Because switches S_{a2} , S_{b2} can only be activated twice in a line period (60Hz) and the switching frequency is larger than the line frequency ($f_s \gg f_m$), the switching losses of the proposed circuit is approximated to $4 V_s f_{s}$. Obviously, the switching power loss is nearly half that of the CCHB inverter. Considering the harmonics in the inverter output voltage V_{AB} , the amplitude of the fundamental and harmonic components in the output voltage V_{AB} are calculated by PSIM software. The phase shift PWM technique is adopted for the CCHB inverter. Both of the CCHB multilevel inverter and the studied multilevel inverter are operated in the same condition, including the same switching frequency 18kHz, the same modulation index m_a , the same input voltage $V_S=100V$ and output L-C filter, $L_o=420\mu H$, $C_o=4.7\mu F$.

III. SIMULATION RESULTS

To facilitate understanding of the operating principle and as verification, a Simulation system with a high step-up DC/DC converter stage and the simplified multilevel DC/AC stage are built with the corresponding parameters listed. The specifications of the two preceding high step-up DC/DC converters are (a) input voltage 30V; (b) controlled output voltage 100V; and (c) switching frequency 85kHz. The corresponding specifications of the simplified multilevel DC/AC inverter stage are (1) output power, $P_o=230W$; (2) input voltage, $V_s=100V$; (3) output voltage, $v_o=110V_{rms}$; (4) line frequency, $f_m=60Hz$; (5) switching frequency, $f_s=40kHz$; and (6) peak modulation index, $m_{peak}=0.76$. For better understanding, the guidelines and considerations of the DC-link capacitance and the use of an L-C output filter at the output are described as follows.

A. Sizing DC-link capacitor

For the discussed two-stage DC/AC conversion system, the DC-link capacitance is sized to keep voltage fluctuations within specified limits to prevent over-voltage on the DC bus.

International Journal of Advanced Research in Electrical, Electronics and Instrumentation Engineering

(An ISO 3297: 2007 Certified Organization)

Vol. 2, Issue 12, December 2013

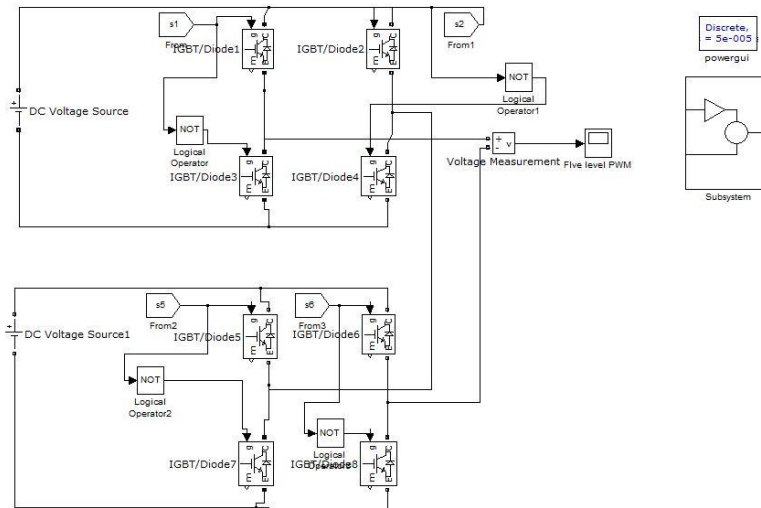


Fig. 3:Simulation diagram of five level inverter

To calculate the relationship between capacitance and voltage limits, the net power flowing into the bus capacitor, i.e. DClink capacitor, is expressed as where P_{DER} is the total output power of the DER modules, and V_o and I_o are the peak AC-side quantities.

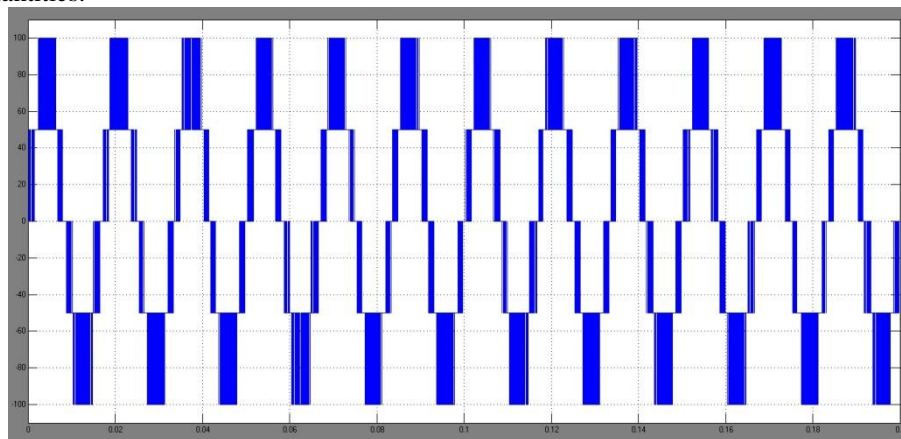


Fig. 4:Wave forms of five level inverter

Assuming a steady-state operating condition whereby the net average power flow is zero, the instantaneous power flow into the bus capacitance C_{bus} is $P_{DER} \cos 2\omega t$. Integrating this expression provides the energy, and equating the peak change in energy stored in the capacitor with where $V_{bus,max}$ is the peak bus voltage, $V_{bus,min}$ is the minimum value of bus voltage, and $C_{bus} = C_{bus1} \times C_{bus2} / (C_{bus1} + C_{bus2})$. The voltage deviation is given by For the discussed two-stage conversion system in this study, a design limit of maximum $\Delta V_{bus} = 10V$ is chosen to keep the bus voltage well within the voltage rating of the semiconductors, which now is typically 200V, and to minimize the third-order harmonic occurring on the output voltage.

International Journal of Advanced Research in Electrical, Electronics and Instrumentation Engineering

(An ISO 3297: 2007 Certified Organization)

Vol. 2, Issue 12, December 2013

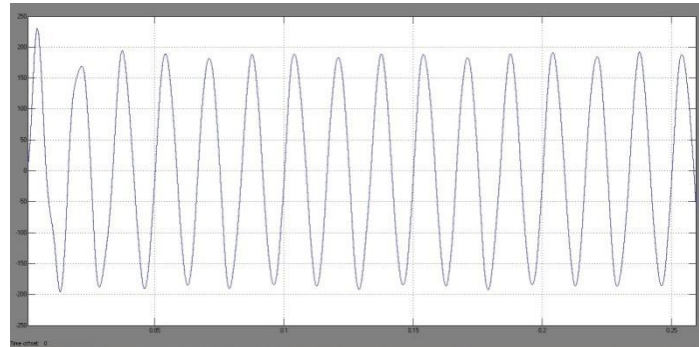


Fig. 5:Output Voltage of five level inverter with filter

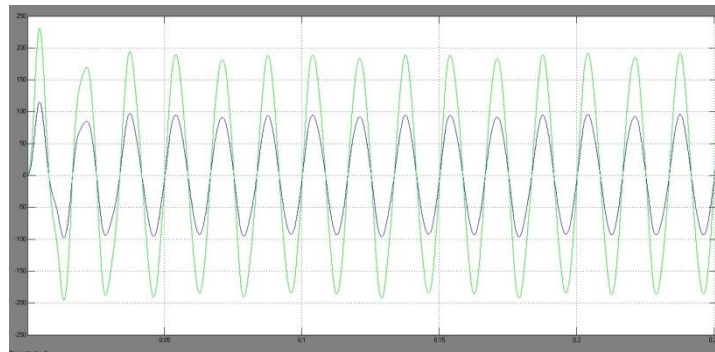


Fig. 6:Output Voltage and Output Current of five level inverter with filter

For the above-mentioned considerations, the capacitance C_{bus1} and C_{bus2} are now chosen as $2000\mu\text{F}$, respectively. It should be noted that, for simplification, the bus capacitance for this case is only selected based on voltage deviation specifications.

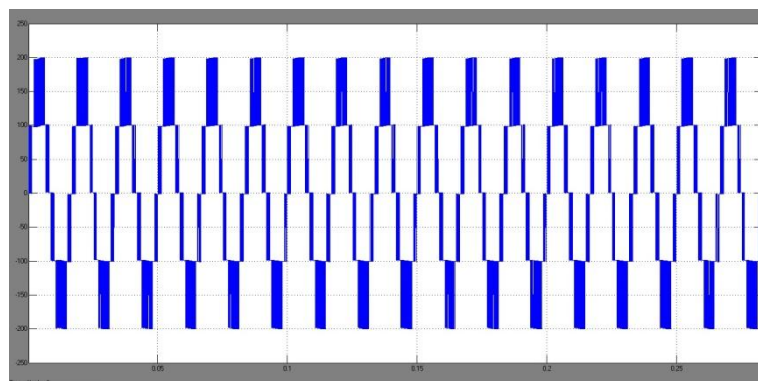


Fig. 6:Output Voltage of five level inverter without filter

B. Choice of output L-C filter

The output L-C filter is tuned to below the switching frequency as follows: where f_{s1} is the switching frequency, and L_o and C_o are inductance and capacitance of the output L-C filter, respectively. The Simulation results of the simplified single-phase inverter stage operated at the rated output power are shown in Figs. 8-10.

International Journal of Advanced Research in Electrical, Electronics and Instrumentation Engineering

(An ISO 3297: 2007 Certified Organization)

Vol. 2, Issue 12, December 2013

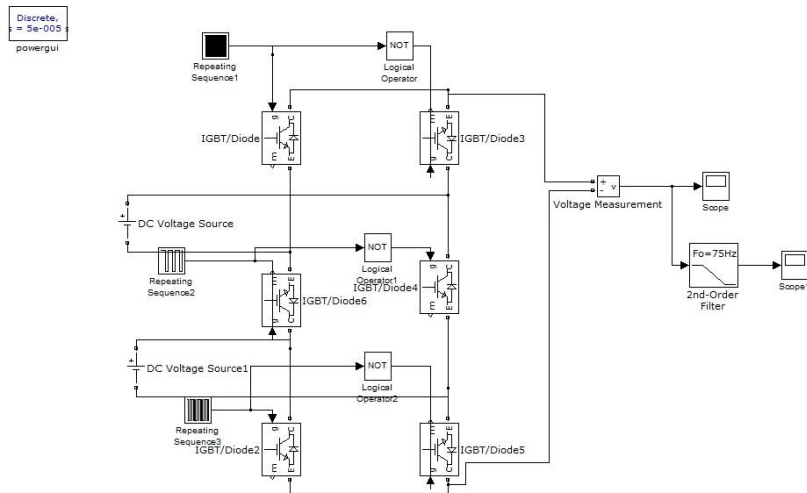


Fig. 7: Simulation diagram of Seven level inverter

Figs. 8-9 show the PWM signals and voltage stresses of the six power switches for the five-level inverter, respectively. It is evident that the voltage stresses of the switches $Sa1$, $Sa3$, $Sb1$, and $Sb3$ are all equal to 100V, and only the other two switches $Sa2$, $Sb2$ must be 200V voltage stress.

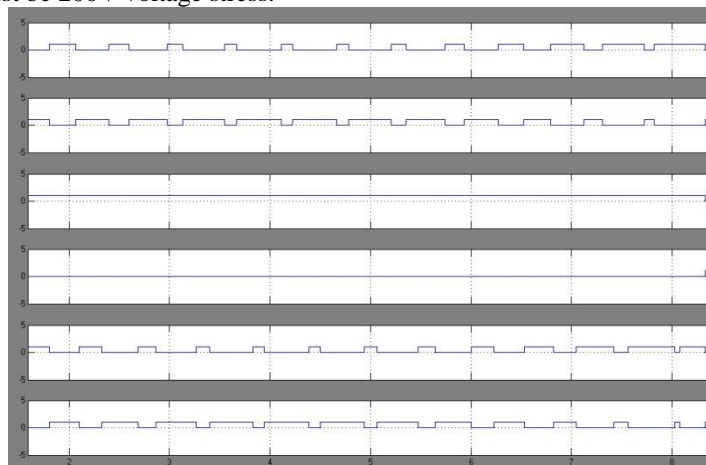


Fig. 8: Switching Pulses of seven level inverter

Fig.9 shows steadystate waveforms of output voltage v_o , output current i_o , and the voltage applied to L-C output filter terminal V_{AB} , respectively, for the inverter with a resistive load of 51Ω.



International Journal of Advanced Research in Electrical, Electronics and Instrumentation Engineering

(An ISO 3297: 2007 Certified Organization)

Vol. 2, Issue 12, December 2013

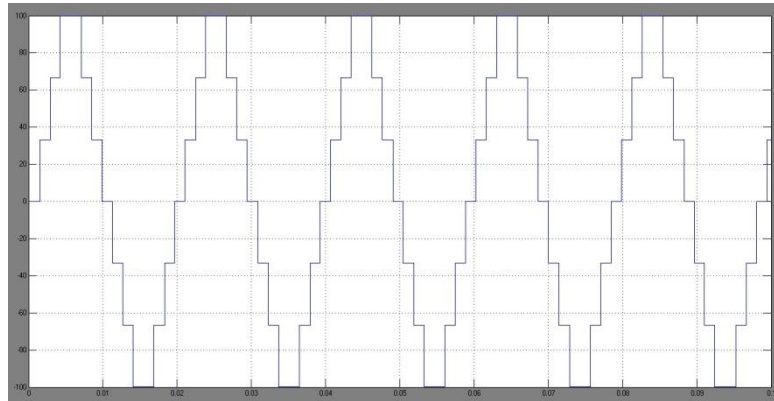


Fig. 9:Output Voltage of seven level inverter

As can be seen in Fig. 8, the waveform shows the desired five voltage levels: 200V, 100V, 0V, -100V, and -200V. The measured RMS value of v_{ois} approximately 110V, while the measured RMS value of i_{ois} is approximately 2.12A. The conversion efficiency of the implemented inverter and THD of the output voltage measured in this case are approximately 96% and 3%, respectively.

IV. CONCLUSION

This work reports a newly-constructed single-phase multistring multilevel inverter topology that produces a significant reduction in the number of power devices required to implement multilevel output for DERs. The studied inverter topology offer strong advantages such as improved output waveforms, smaller filter size, and lower EMI and THD. Simulation results show the effectiveness of the proposed solution. This paper presents a new Novel Asymmetrical Multistring multilevel converter. Here we proposed single phase and three phase multistring multilevel inverters, the proposed converter produces more voltage levels with less number of switches compared to H- bridge configuration. This will reduce the switching losses and number of gate drivers and protection circuits which in turn reduces the cost and complexity of the circuit. Finally a three phase model of the proposed circuit is shown and simulation results are presented.

REFERENCES

- [1] Y. Li, D. M. Vilathgamuwa, and P. C. Loh, "Design, analysis, and realtime testing of a controller for multibus microgrid system," *IEEE Trans. Power Electronics*, vol. 19, no. 5, pp. 1195-1204, Sept. 2004.
- [2] N. Hatziaargyriou, H. Asano, R. Irvani, and C. Marnay, "Microgrids," *IEEE Power and Energy Magazine*, vol. 5, no. 4, pp. 78-94, Jul./Aug. 2007.
- [3] F. Katiraei, R. Irvani, N. Hatziaargyriou, and A. Dimeas, "Microgrids management," *IEEE Power and Energy Magazine*, vol. 6, no. 3, pp. 54-65, May/Jun., 2008.
- [4] C. L. Chen, Y. Wang, J. S. Lai, Y. S. Lee, and D. Martin, "Design of parallel inverters for smooth mode transfer microgrid applications," *IEEE Trans. Power Electronics*, vol. 25, no. 1, pp. 6-15, Jan. 2010.
- [5] C. T. Pan, C. M. Lai, and M. C. Cheng, "A novel high step-up ratio inverter for distributed energy resources (DERs)," *IEEE International Power Electronics Conference-ECCE Asia*, pp.1433-1437, 2010.
- [6] C. T. Pan, C. M. Lai, and M. C. Cheng "A novel integrated single-phase inverter with an auxiliary step-up circuit for low-voltage alternative energy source application," *IEEE Trans. Power Electronics*, vol. 25, no. 9, pp. 2234-2241, Sep. 2010.
- [7] F. Blaabjerg, Z. Chen, and S. B. Kjaer, "Power electronics as efficient interface in dispersed power generation systems," *IEEE Trans. Power Electronics*, vol. 19, no. 5, pp. 1184-1194, Sep. 2004.
- [8] D. G. Infield, P. Onions, A. D. Simmons, and G. A. Smith, "Power quality from multiple grid-connected single-phase inverters," *IEEE Trans. Power Delivery*, vol. 19, no. 4, pp. 1983-1989, Oct. 2004.
- [9] S. B. Kjaer, J. K. Pedersen, and F. Blaabjerg "A review of single-phase grid-connected inverters for photovoltaic modules," *IEEE Trans. Industry Applications*, vol. 41, no. 5, pp. 1292-1306, Sep./Oct. 2005.
- [10] O. Lopez, R. Teodorescu, and J. Doval-Gandoy, "Multilevel transformerless topologies for single-phase grid-connected converters" *IEEE Industrial Electronics Conference*, pp. 5191-5196, 2006.
- [11] T. Kerekes, R. Teodorescu, and U. Borup, "Transformerless photovoltaic inverters connected to the grid," *IEEE Applied Power Electronics Conference*, pp. 1733-1737, 2007.
- [12] G. Ceglia, V. Guzman, C. Sanchez, F. Ibanez, J. Walter, and M. I. Gimenez, "A new simplified multilevel inverter topology for DC-AC conversion," *IEEE Trans. Power Electronics*, vol. 21, no. 5, pp. 1311- 1319, Sep. 2006
- [13] N. A. Rahim and J. Selvaraj, "Multistring five-level inverter with novel PWM control scheme for PV application," *IEEE Trans. Power Electronics*, vol. 57, no. 6, pp. 2111-2123, Jun. 2010



International Journal of Advanced Research in Electrical, Electronics and Instrumentation Engineering

(An ISO 3297: 2007 Certified Organization)

Vol. 2, Issue 12, December 2013

- [14] C. T. Pan, W. C. Tu, and C. H. Chen, "A novel GZV-based multilevel single phase inverter," *Taiwan Power Electronics conference*, pp. 1391-1396, Sep. 2010.
- [15] W. Yu, J. S. Lai, H. Qian, C. Hutchens, J. Zhang, G. Lisi, A. Djabbari, G. Smith, and T. Hegarty, "High-efficiency inverter with H6-type configuration for photovoltaic non-isolated AC module applications," *IEEE Applied Power Electronics Conference and Exposition*, pp. 1056-1061, 2010.
- [16] S. Vazquez, J. I. Leon, J. M. Carrasco, L. G. Franquelo, E. Galvan, M. Reyes, J. A. Sanchez, and E. Dominguez, "Analysis of the power balance in the cells of a multilevel cascaded H-bridge converter," *IEEE Trans. Industrial Electronics*, vol. 57, no. 7, pp. 2287-2296, Jul. 2010.
- [17] S. Daher, J. Schmid, and F. L.M. Antunes, "Multilevel inverter topologies for stand-alone PV systems," *IEEE Trans. Industrial Electronics*, vol. 55, no. 7, pp. 2703-2712, Jul. 2008.

BIOGRAPHY



B. Suresh Kumar born in India. Hereceived B.Tech (Electrical and Electronics Engineering) degree from PrakasamEngineering College Kandukur, JNTU Kakinada. He is pursuing M.Tech (Power Electronics) in Chirala Engineering College at Chirala affiliated to JNTU Kakinada. His area of research is in Power Electronics and Solar Power Systems.



GantaJoga Raowas born in srikakulam, Andhra Pradesh, India, in 1983.He received B.Tech (Electrical & Electronics Engineering)degree from Kamala Institute of Technology & Science, Jawaharlal Nehru Technological University, Hyderabad, India, in 2004 and the M.Tech degree from Jawaharlal Nehru Technological University College, Hyderabad ,India in 2007. He is working as associate professor in the department of Electrical &Electronics Engineering in Chirala Engineering College, Chirala, Andhra Pradesh. His area of interest Includes power electronics, electrical machines and drives, Digital control systems, HVDC.Mr. G.JOGA RAO is a Life Member of the Indian Society for Technical Education (LMISTE).